Hindawi Publishing Corporation
Abstract and Applied Analysis
Volume 2013, Article ID 207987, 8 pages
http://dx.doi.org/10.1155/2013/207987

*Research Article*

# Ecological Vulnerability Assessment Integrating the Spatial Analysis Technology with Algorithms: A Case of the Wood-Grass Ecotone of Northeast China

**Zhi Qiao,[1] Xi Yang,[2] Jun Liu,[2,3] and Xinliang Xu[3]**

[1] *State Key Laboratory of Water Environment Simulation, School of Environment, Beijing Normal University, No. 19, Xinjiekouwai Street, Beijing 100875, China*
[2] *College of Geography and Tourism, Chongqing Normal University, No.12, TianChen Road, ShaPingBa District, Chongqing 400047, China*
[3] *Institute of Geographic Sciences and Natural Resources Research, Chinese Academy of Sciences, A11 DaTun Road, ChaoYang District, Beijing 100101, China*

Correspondence should be addressed to Jun Liu; liujun_igsnrr@yahoo.com.cn

Received 25 February 2013; Accepted 27 March 2013

Academic Editor: Jianhong (Cecilia) Xia



This study evaluates ecological vulnerability of the wood-grass ecotone of northeast China integrating the spatial analysis technology with algorithms. An assessment model of ecological vulnerability is developed applying the Analytical Hierarchy Process. The composite evaluation index system is established on the basis of the analysis of contemporary status and potential problems in the study area. By the application of the evaluation model, ecological vulnerability index is calculated between 1990 and 2005. The results show that ecological vulnerability was mostly at a medium level in the study area, however the ecological quality was deteriorating. Through the standard deviational ellipse, the variation of ecological vulnerability can be spatially explicated. It is extremely significative for the prediction of the regions that will easily deteriorate. The deterioration zone was concentrating in the area of Da Hinggan Ling Mountain, including Xingan League, Chifeng, Tongliao, and Chengde, whereas the improvement zone was distributing in the north-central of Hulunbeier.

## 1. Introduction

Ecosystem provides the essential material that is indispensable for human subsistence and development [1]. Nevertheless, the ecosystem has been taking a turn for the worse, which results from both the global change and population growth [2]. The ecosystem exhibits a significant amount of characters that are subjected to the exotic environment as the ecological vulnerability. Some investigators conceptualized ecological vulnerability as a function of exposure, sensitivity, and adaptive capacity [3, 4]. The definition is valuable as it embraces its own characters for ecosystem, that is, experiencing internal or external system disturbance [5], the ability of a system to adjust its behavior and characteristics in order to enhance its capacity versus external stress [6], and the establishing principle of ecological vulnerability index system [7].

The assessment of ecological vulnerability is progressively important as it enables us to ascertain the potential problem and to stimulate eco-environment protection [8]. The origins of vulnerability assessment are social sciences and economic field; however there has been an increasing interest in the ecosystem over the last decades [9]. Numerous approaches are employed for the assessment of ecological vulnerability, for example, comprehensive evaluation method [10], indices weight method (IWM) [11], analytical hierarchy process (AHP) [10, 12], and spatial principal component analysis model (SPCA) [2]. The integration of spatial analysis technology with algorithms provides a powerful means for ecological vulnerability assessment and forecast. Many spatially explicit indicators of sensitivity, exposure and adaptive capacity are available, all of which are essential to ecological vulnerability

assessment and forecast, through mining from geographic information system (GIS) and remote sensing (RS).

The wood-grass ecotone of Northeast China is initially proposed as a vulnerable area by the Ministry of environmental protection of the People's Republic of China in 2008 [13]. So far, experiments on ecological vulnerability of the wood-grass ecotone were insufficient. Specifically, we concentrate on the subsequent issues: (1) What was the spatial-temporal variation of ecological vulnerability in the region between 1990 and 2005? (2) How does integrate spatial analysis technology and algorithms for ecological vulnerability assessment and forecast?

## 2. Study Area

The wood-grass ecotone of Northeast China, lying in between the Da Hinggan Ling mountain and Yanshan mountain, extends about 14 degrees of latitude (39°30′~53°20′N) and 11 degrees of longitude (115°02′ ~ 126°04′E). It contains six cities: Hulunbeier, Xingan League, Tongliao, Chifeng, Chengde, Zhangjiakou, with the area about $5.24 \times 10^5$ km$^2$ and the altitude 89~2683 m (Figure 1). Ecological problems, for instance, ecological transition characteristics and heterogeneity, grassland degeneration, and soil erosion [13], have seriously affected sustainable development of the region. More significant is the truth that the entire area plays as an ecological security barrier for Beijing, which is the capital of China.

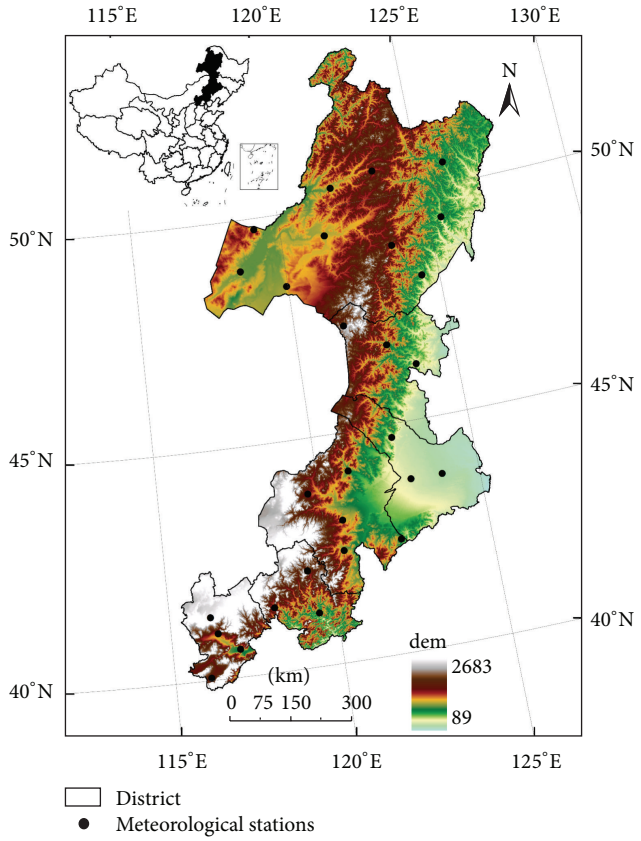


Figure 1: Distribution of the wood-grass ecotone of Northeast China.

## 3. Materials and Methods

The process of ecological vulnerability assessment involves the subsequent phases, that is, establishment of ecological vulnerability index system, modeling the assessment of ecological vulnerability, index calculation and standardization, ecological vulnerability assessment and classification, and variation analysis of ecological vulnerability (Figure 2).

*3.1. Establishment of Ecological Vulnerability Index System.* The study intends to measure the ecological vulnerability of the wood-grass ecotone of Northeast China. Through the investigation of contemporary status and potential problems of the study area, we summarize the characteristics as follows. Elevation and slope have a remarkable influence on the ecosystem because it lies in a mountainous area. The content of soil organic matter is 7%~10% in the east and middle regions; however it is only 0.5%~2% in the west. As a result of the infertile soil and thin soil layer, the soil is undoubtedly encroached by rain and wind. In addition, the overburdened agricultural activities seriously damage essentially vulnerable environment as a result of reclaiming forest and grass land. Considering the above investigations and combining with other research achievements carried out in the past few decades for the assessment of ecological vulnerability [1, 2, 14], eight elements are chosen in order to synthetically evaluate ecological vulnerability of the wood-grass ecotone of Northeast China. These components involve LUCC, DEM, soil texture, soil organic matter, precipitation, annual accumulated temperature (≥0°C), windy days in winter and spring (>6 m/s), and NDVI (Table 1). The above data used in the study are derived from Landsat thematic mapper (TM) image, digital elevation model (DEM), national soil field survey data, and meteorological data. The LUCC data is manually interpreted based on TM images, and there are six aggregated classes of land use, that is, cropland, forest, grassland, water body, bare land, and built-up land [15].

*3.2. Modeling the Assessment of Ecological Vulnerability.* Besides the establishment of ecological vulnerability index system, the additional key for the assessment of ecological vulnerability is determining the weight of individual evaluation indicator. In this paper, analytic hierarchy process (AHP) [16] is applied to generate a comprehensive decision for the assessment of ecological vulnerability.

The paper aims to make an assessment of ecological vulnerability; therefore the destination layer (level 1) is the ecological vulnerability index. The evaluation factors (level 2) for the criterion layer are *ecological suitability index*, *landscape pattern index*, and *land resources utilization degree index*. The corresponding quantitative indices (level 3) are *soil erosion sensitivity index* and *soil desertification sensitivity index*, *landscape unit plaques density* and *landscape evenness index*, and *land utilization degree composite index* (Table 1). The above system includes natural factors and anthropogenic

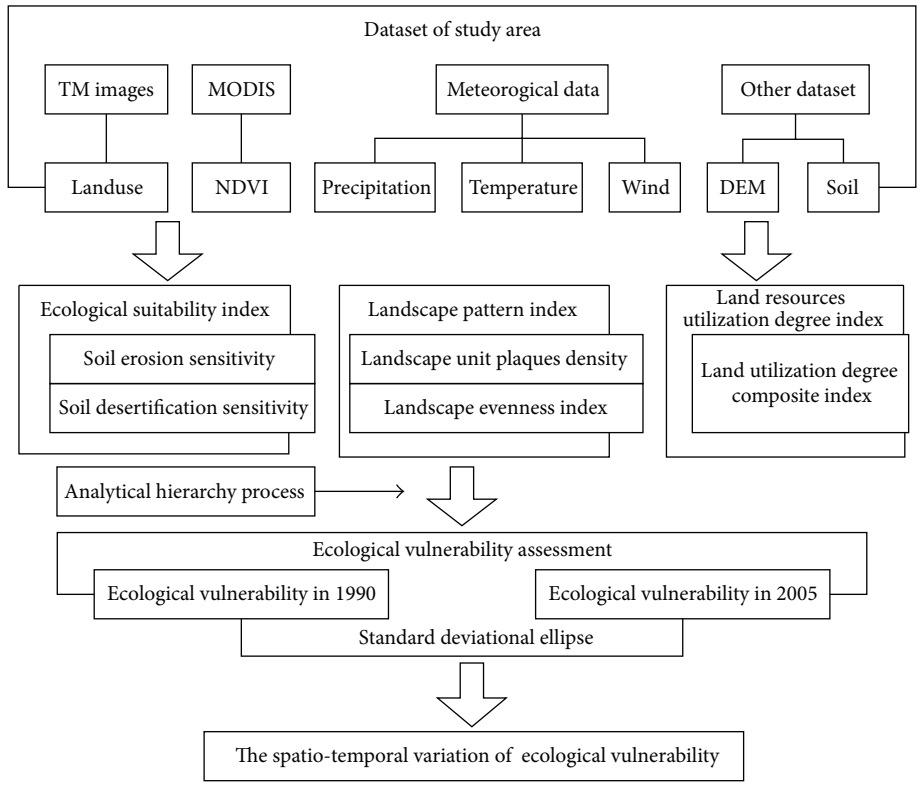


Figure 2: The workflow of ecological vulnerability assessment.

factors that directly relate with contemporary status and potential problems in the study area.

### 3.3. Index Calculation and Standardization

*3.3.1. Ecological Suitability Index.* Ecological suitability is determined by ecological sensitive degree of ecosystem. Sensitivity analysis is to distinguish the area which it is easily deteriorated by exotic environment. Sensitivity analysis is comprised of soil erosion sensitivity and soil desertification sensitivity on the basis of contemporary status and potential problems in the study area. Soil erosion sensitivity is determined by precipitation, DEM, soil, and LUCC. Soil desertification sensitivity is evaluated by average precipitation, annual accumulated temperature (≥0°C), windy days in winter and spring (>6 m/s), and NDVI.

(a) *Soil Erosion Sensitivity.* In the paper, we use the Wischmeier empirical formula to calculate the rainfall erosivity ($R$) [17]:

$$R = \sum_{i=1}^{i=12} 1.735 \times 10^{(1.5\log(P_i^2/P)-0.8188)}, \quad (1)$$

where $R$ is the rainfall erosivity factor and its unit is MJ·mm·ha$^{-1}$·h$^{-1}$·year$^{-1}$, $P_i$ is monthly rainfall in mm, and $P$ is annual rainfall in mm.

Topographic factor ($LS$) is to estimate the relationship between topographical relief and soil erosion sensitivity.

Table 1: The ecological vulnerability index system of the wood-grass ecotone of Northeast China.

| Destination layer | Criterion layer | Index layer | Data source |
|---|---|---|---|
| Ecological vulnerability | Ecological suitability index | Soil erosion sensitivity index | Precipitation |
| | | | DEM |
| | | | Soil texture |
| | | | Soil organic matter |
| | | | LUCC |
| | | Soil desertification sensitivity index | Precipitation |
| | | | Annual accumulated Temperature (≥0°C) |
| | | | Windy days in winter and spring (>6 m/s) |
| | | | NDVI |
| | Landscape pattern index | Landscape unit plaques density | LUCC |
| | | Landscape evenness index | |
| | Land resources utilization degree index | Land utilization degree composite index | |

Table 2: Soil erosion sensitivity standard classification.

| Index | Slight sensitivity | Light sensitivity | Medium sensitivity | Heavy sensitivity | Extreme sensitivity |
|---|---|---|---|---|---|
| $R$ | ≤25 | 25–100 | 100–400 | 400–600 | >600 |
| LS | ≤20 | 20–50 | 51–100 | 101–300 | >300 |
| $K$ | ≤0.08 | 0.08–0.12 | 0.12–0.2 | 0.2-0.3 | 0.3–0.45 |
| CM | Water, herb swamp, rice paddies | Broad-leaved forest, coniferous forest, grass, bush forest | Shrub grassland, double cropping crop | Desert, once cropping crop | No vegetation |
| Value | 1 | 3 | 5 | 7 | 9 |
| Classification value (SS) | 1.0–2.0 | 2.1–4.0 | 4.1–6.0 | 6.1–8.0 | >8.0 |

Table 3: Soil desertification sensitivity standard classification.

| Index | Slight sensitivity | Light sensitivity | Medium sensitivity | Heavy sensitivity | Extreme sensitivity |
|---|---|---|---|---|---|
| Moisture degree index | >0.65 | 0.5–0.65 | 0.20–0.50 | 0.05–0.20 | <0.05 |
| Windy days in winter and spring (>6 m/s) | <15 | 15–30 | 30–45 | 45–60 | >60 |
| Soil texture | Pedestal rock | Viscidity | Gravel | Loamy texture | Sandiness |
| Vegetation cover | Dense | Moderate | Low | Thin | Bare land |
| Value | 1 | 3 | 5 | 7 | 9 |
| Classification value (DS) | 1.0–2.0 | 2.1–4.0 | 4.1–6.0 | 6.1–8.0 | >8.0 |

The paper uses the move window of 5 km × 5 km to extract the surface rolling on the basis of DEM.

The soil erodibility factor ($K$) is calculated through the following equation [18]:

$$K = \left\{0.2 + 0.3\exp\left[-0.0256S_a\left(1 - \frac{S_i}{100}\right)\right]\right\} \times \left(\frac{S_i}{C_l + S_i}\right)^{0.3} \times \left[1 - \frac{0.25C}{C + \exp(3.72 - 2.95C)}\right] \times \left[1 - \frac{0.7S_n}{S_n + \exp(-5.51 + 22.9S_n)}\right], \quad (2)$$

where $K$ is soil erodibility factor and its unit is $t\cdot ha^{-1}\cdot h\cdot MJ^{-1}\cdot mm^{-1}\cdot ha^{-1}$. $S_a$, $S_i$ and $C_l$ is the percentage of sand, powder, and clay content in soil. $S_n = 1 - S_a/100$. $C$ is carbon content in soil; it is the value of that organic content multiplied by *Bemmelen* (0.58 g C/g SOC) [19].

Cropping management factor (CM) is the factor used most often to compare the relative impacts of management options on conservation plans. It is then an estimate of the ratio of soil loss under actual conditions to losses experienced under the reference conditions. Because of the diversity of the type of the land cover and the administrative manner, the ability of the prevention of soil erosion is different (Table 2).

In summary, the calculation method of soil erosion sensitivity index is as follows:

$$SS = \sqrt[4]{\prod_{i=1}^{4} C_i}, \quad (3)$$

where SS is soil erosion sensitivity index, $C_i$ is the value of each sensitivity factor, and $i$ is the sensitivity factor (Table 2) [13].

(b) *Soil Desertification Sensitivity.* Similarly, the calculation method of soil desertification sensitivity is shown as follows:

$$DS = \sqrt[4]{\prod_{i=1}^{4} D_i}, \quad (4)$$

where DS is soil desertification sensitivity, $D_i$ is the value of each sensitivity factor, and $i$ is the sensitivity factor. In the paper, we use moisture degree index, soil texture, windy days in winter and spring, and vegetation cover to evaluate the soil desertification sensitivity (Table 3).

The subsequent equation is applied to calculate the moisture degree index, that is, the annual total precipitation ($r$) divides by annul accumulated temperature (≥0°C), $\sum\theta$,

$$K = \frac{r}{0.1 \times \sum\theta}. \quad (5)$$

Wind speed is took notes at each meteorological station; we interpolate those materials to count the windy days in winter and spring (>6 m/s) in the entire region.

According to the responce of soil texture to soil desertification sensitivity, the soil type is classified into five grades through international soil texture triangle table.

Vegetation cover shows the capability of preventing desertification. The greater the vegetation cover, the stronger the ability of prevention function. We use $f$ to show vegetation cover

$$f = \frac{NDVI - NDVI_{min}}{NDVI_{max} - NDVI_{min}}, \quad (6)$$

where $f$ is the vegetation cover, NDVI is normalized difference vegetation index, $\mathrm{NDVI}_{\min}$ is the minimum value of NDVI, and $\mathrm{NDVI}_{\max}$ is the maximum value of NDVI.

*3.3.2. Landscape Pattern Index*

(a) *Landscape Unit Patch Density (PD).* Patch density is a limited, but fundamental, aspect of landscape pattern. PD has the same basic utility as the number of patches as an index, except that it expresses the number of patches on a per unit area basis that facilitates comparisons among landscapes of varying size. We calculate PD with the following expression:

$$\mathrm{PD} = \frac{N}{A}, \tag{7}$$

where PD is landscape unit patch density, $N$ is the patch number of each landscape, and $A$ is the area of each landscape.

(b) *Landscape Evenness Index (SHEI).* SHEI equals minus the sum, across all patch types, of the proportional abundance of each patch type multiplied by that proportion, divided by the logarithm of the number of patch types. In other words, the observed Shannon's diversity index divided by the maximum Shannon's diversity index for that number of patch types. We calculate the landscape unit plaques density with the following expression:

$$\mathrm{SHEI} = \frac{-\sum_{i=1}^{m} \left(P_i \times \ln P_i\right)}{\ln m}, \tag{8}$$

where $P_i$ is the proportion of the landscape occupied by patch type $i$. $m$ is the number of patch types present in the landscape. SHEI = 0 when the landscape contains only 1 patch (i.e., no diversity) and approaches 0 as the distribution of area among the different patch types becomes increasingly uneven (i.e., dominated by 1 type). SHEI = 1 when distribution of area among patch types is perfectly even (i.e., proportional abundances are the same).

*3.3.3. Land Resources Utilization Degree Index.* Land resources utilization degree is expressed as the land utilization degree composite index. The connotation of land resources utilization degree that presents as the response indicator of ecological vulnerability is the limit of the land resource. The superior limit is the maximum degree of utilization of land resources, which means that it is not able to further develop the land resource, and vice versa. Where the value of bare land is 1, the value of forest, grass, and water body is 2, the value of cropland is 3, and the value of built-up land is 4, respectively.

*3.3.4. Index Standardization.* There are significant differences and diverse units for evaluation indicators. It is difficult to further evaluate ecological vulnerability through these heterogeneous indices indirectly. The value of evaluation indices must be standardized in a uniform measurement system

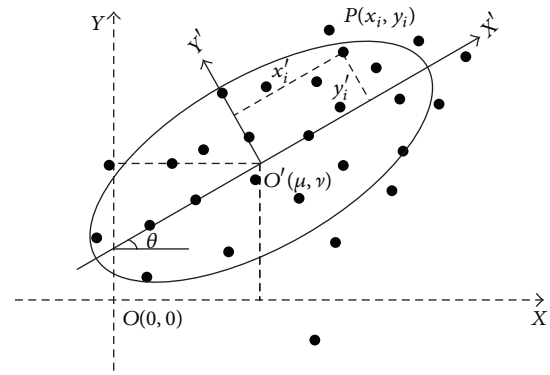


Figure 3: Standard deviational ellipse.

$$X'_{ij} = \frac{X_{ij} - X_{\min,j}}{X_{\max,j} - X_{\min,j}}, \tag{9}$$

where $X'_{ij}$ represents the standardized value of factor $j$ in grid $i$, $X_{ij}$ represents the original value of factor $j$ in grid $i$, $X_{\max,j}$, and $X_{\min,j}$ represent the maximum and minimum value of factor $j$ in grid $i$, respectively.

*3.4. Ecological Vulnerability Assessment and Classification.* According to the evaluation factors and their weights calculated by analytical hierarchy process, ecological vulnerability index (EVI) is calculated as follows:

$$\mathrm{EVI} = \alpha \cdot \mathrm{SS} + \beta \cdot \mathrm{DS} + \gamma \cdot \mathrm{PD} + \omega \cdot \mathrm{SHEI} + \phi \cdot \mathrm{La}, \tag{10}$$

where EVI is ecological vulnerability index, SS, DS, PD, SHEI, and La are, respectively, soil erosion sensitivity index, soil desertification sensitivity index, landscape unit patch density, landscape evenness index, and land utilization degree composite index, and $\alpha$, $\beta$, $\gamma$, $\omega$, and $\phi$ are the weight values of each evaluative factor, respectively.

The scores of EVI scatter between 0 (the lowest grade) and 1 (the highest grade). To further reveal the characteristics of ecological vulnerability, we reclassify the grade of ecological vulnerability through the ArcGIS software and following natural breaks classification. The standard of ecological vulnerability is slight (0–0.2), light (0.2–0.4), medium (0.4–0.6), heavy (0.6–0.8), and extreme (0.8–1).

*3.5. Variation Analysis of Ecological Vulnerability Based on the Standard Deviational Ellipse.* Although there are numerous methods and cases of ecological vulnerability assessment, studies on forecasting ecological vulnerability are insufficient. The paper aims to forecast spatial variation of ecological vulnerability on the basis of the standard deviational ellipse.

The standard deviational ellipse aims to evaluate the trend of a set of points (Figure 3). The work includes two steps: ascertaining the mean center and determining the dispersion of the scattered points [20, 21].

Firstly, move the original coordinate system to the mean center $(\mu, \nu)$ of the set of $n$ units studied

$$\mu = \frac{\sum_{i=1}^{n} x_i}{n}, \qquad \nu = \frac{\sum_{i=1}^{n} y_i}{n}, \tag{11}$$

where $\mu$, $\nu$ are the mean value of $x_i$, $y_i$ in the original coordinate system ($XOY$), respectively.

Then calculate the standard deviation ($\sigma_{y'}$) of the $y$ coordinates of the units,

$$\sigma_{y'} = \sqrt{\sum_{i=1}^{n} \frac{\left(y_i'\right)^2}{n}}, \tag{12}$$

where $y_i'$ is the coordinate of the units in the transformed coordinate system $X'O'Y'$. Similarly, $x_i'$ is calculated as the above method.

Finally, rotate the coordinate system $XOY$ about the new origin $(\mu, \nu)$ by angle $\theta$ $(0 < \theta \leq 2\pi)$ and calculate the standard deviation ($\sigma_{y'}$) of the $Y'$ coordinates again,

$$\sigma_{y'} = \sqrt{\frac{\sum_{i=1}^{n} \overline{y_i}^2 \cos^2\theta - 2\sum_{i=1}^{n} \overline{x_i}\,\overline{y_i} \sin\theta\cos\theta + \sum_{i=1}^{n} \overline{x_i}^2 \sin^2\theta}{n}}, \tag{13}$$

where $\overline{x_i}$ and $\overline{y_i}$ are the coordinates of the units in the rotated coordinate system $X'O'Y$ and $\sigma_{y'}$ is the standard deviation of the $Y'$ coordinates. A study of the foregoing equations shows that the locus of the $\sigma_{y'}$ value as the axis rotates about the mean center is an ellipse. In order to plot the ellipse on the map, it is necessary to locate the major and minor axes and to calculate the corresponding $\sigma_{y'}$ values.

When the $\sigma_{y'}$ value obtains the minimum value in the rotated coordinate system, the rotated angle $\theta$ is the direction of scattered points. Then it can get the minimum value through calculating the derivative of $\sigma_{y'}$ for (12)

$$\frac{d\sigma_{y'}}{d\theta} = \frac{1}{n\sigma_{y'}}\left[\sum_{i=1}^{n} \overline{x_i}^2 \sin\theta\cos\theta - \sum_{i=1}^{n} \overline{x_i}\,\overline{y_i}\left(\cos^2\theta - \sin^2\theta\right) - \sum_{i=1}^{n} \overline{y_i}^2 \sin\theta\cos\theta\right]. \tag{14}$$

Solving for $\theta$,

$$\tan\theta = \frac{\left(\sum_{i=1}^{n} \overline{x_i}^2 - \sum_{i=1}^{n} \overline{y_i}^2\right) \pm \sqrt{\left(\sum_{i=1}^{n} \overline{x_i}^2 - \sum_{i=1}^{n} \overline{y_i}^2\right)^2 + 4\left(\sum_{i=1}^{n} \overline{x_i}\,\overline{y_i}\right)^2}}{2\sum_{i=1}^{n} \overline{x_i}\,\overline{y_i}}. \tag{15}$$

If $\theta$ value is substituted for the variable in (13) and (14), the maximum and minimum $\sigma_{y'}$ values are given. These are the semimajor and semiminor axes of the standard deviational ellipse. The $\theta$ value shows the distribution of scattered points.

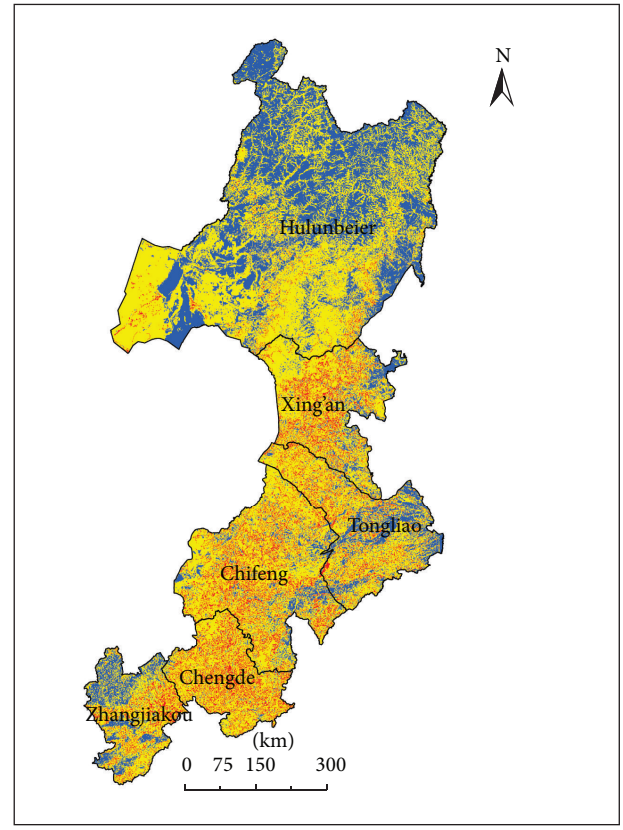


Figure 4: Spatial distribution of ecological vulnerability in 2005.

## 4. Result Analyses

*4.1. The Assessment of Ecological Vulnerability in 2005.* The ecological vulnerability of the wood-grass ecotone of northeast China is calculated according to the above method in Section 3.3. The largest area was medium-vulnerability zone, which accounted for 59.97% and mainly distributed in Hulunbeier and Chengde, followed by light-vulnerability zone accounted for 28.99%. Heavy-vulnerability zone accounted for 11.04%, and it was principally allocated in Chengde, Chifeng, Xingan League, and Zhangjiakou (Figure 4).

*4.2. The Spatio-Temporal Variation of Ecological Vulnerability between 1990 and 2005.* Statistical analysis indicates that areas of medium-vulnerability zone and heavy-vulnerability zone both increased between 1990 and 2005. Medium-vulnerability zone increased from 42.44% to 59.97%, which had the fastest growth among all zones. It is worthwhile to note that heavy-vulnerability zone increased by 5.64 $\times$ $10^4$ km$^2$, and the percentage increased from 0.27% to 11.04%. Light vulnerability zone decreased from 56.98% to 28.99%, which had the fastest reduction among all zones. Taken altogether, ecological quality was deteriorating during

Table 4: Variation matrix of the ecological vulnerability between 1990 and 2005 ($km^2$).

| Ecological vulnerability | Slight | Light | Medium | Heavy |
|---|---|---|---|---|
| Slight | 0 | 1634 | 0 | 0 |
| Light | 0 | 117882 | 163287 | 17442 |
| Medium | 0 | 32411 | 150476 | 39531 |
| Heavy | 0 | 0 | 530 | 883 |

1990~2005. Transfer area from slight-vulnerability zone to light-vulnerability zone was 1634 $km^2$. Light-vulnerability zones converted into medium-vulnerability zone by $1.63 \times 10^5$ $km^2$, and light-vulnerability zones converted into heavy-vulnerability zone by $1.74 \times 10^4$ $km^2$, which accounted for 55% and 6% of the area of light vulnerability in 1990, respectively (Table 4).

Transfer zones can be explored through the standard deviational ellipse. There were six kinds of variations in the study area. Hence we use different colors to display those variations (Figure 5). There were four kinds of variations that indicate deterioration for ecological environment and other two kinds of variations that illustrate improvement for ecological environment. For the four kinds of deterioration zones, the zone changing from slight-vulnerability to light-vulnerability zone appeared in the southwest of Hulunbeier. And the other three deterioration zones concentrated in the Da Hinggan Ling mountain, including Xingan League, Chifeng, Tongliao, and Chengde. It showed that ecological circumstance was the absence of stabilization; both anthropogenic activity further endangered the environment in these regions. Corresponding measures must be taken to protect those deterioration zones. The improvement zone predominantly distributed in the north central of Hulunbeier, simultaneously.

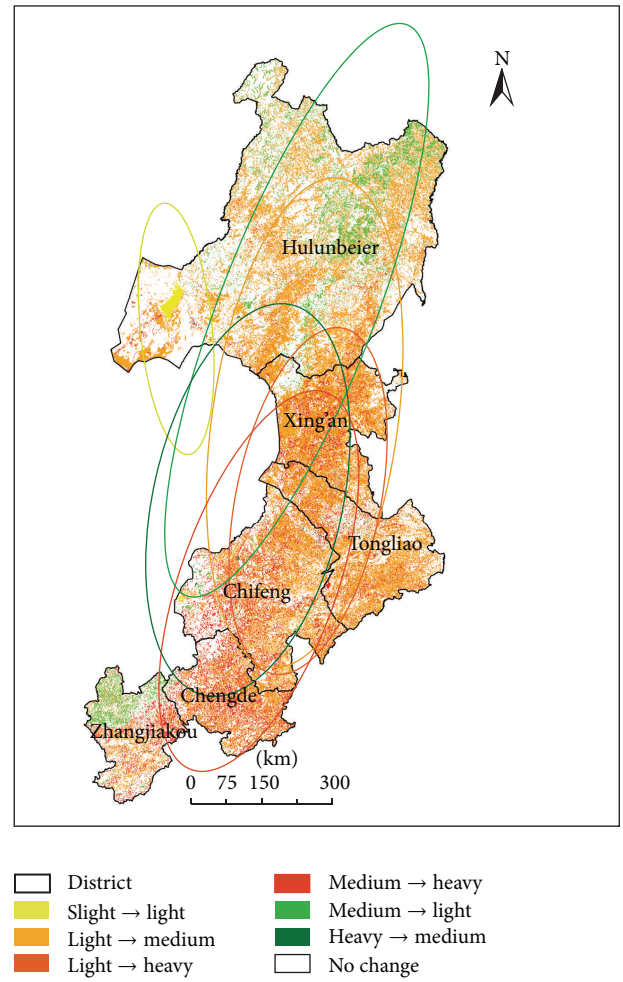


Figure 5: Spatial distribution of ecological vulnerability changes.

## 5. Discussions and Conclusions

Comparing spatio-temporal variation of the ecological vulnerability, the area of medium-vulnerability zone and heavy-vulnerability zone increased, simultaneously; the area of slight-vulnerability zone and light-vulnerability zone decreased. It was emphasized that the ecological quality became worse between 1990 and 2005 in the wood-grass ecotone of northeast China. There were numerous reasons impacting the spatio-temporal variation of ecological vulnerability, that is, global climate change, vegetation degradation, soil erosion, topographical relief, and rapid population growth.

The standard deviational ellipse is positive to spatially explore and forecast the deterioration zones. In the middle and south of the study area, the ecological environment deteriorated. At the same time, the ecological environment got better in the north of the study area. The method is also important as it is of significant benefit to identify areas at risk that will threaten sustainable development. Of course, the method can similarly discover areas where the quality of ecological environment is improving in virtue of the implementation of environmental protection. This study indicates that the assessment of ecological vulnerability can be improved with high spatio-temporal resolution through integrating GIS and RS with algorithms. It is more likely to be accepted by the local governments who would implement the recommended policies.

## Acknowledgments

This study was supported by the National Natural Science Foundation of China (NSFC, no. 41101115) and Key Technologies R&D Program of China (2013BAC04B03).

## References

[1] P. H. Qiu, S. J. Xu, G. Z. Xie, B. N. Tang, H. Bi, and L. S. Yu, "Analysis of the ecological vulnerability of the western Hainan Island based on its landscape pattern and ecosystem sensitivity," *Acta Ecologica Sinica*, vol. 27, no. 4, pp. 1257–1264, 2007.

[2] S. Y. Wang, J. S. Liu, and C. J. Yang, "Eco-environmental vulnerability evaluation in the Yellow River Basin, China," *Pedosphere*, vol. 18, no. 2, pp. 171–182, 2008.

[3] H. Eakin and A. L. Luers, "Assessing the vulnerability of social-environmental systems," *Annual Review of Environment and Resources*, vol. 31, pp. 365–394, 2006.

[4] G. C. Gallopín, "Linkages between vulnerability, resilience, and adaptive capacity," *Global Environmental Change*, vol. 16, no. 3, pp. 293–303, 2006.

[5] J. J. MaCarthy, O. F. Canziani, N. A. Leary, D. J. Dokken, and K. S. White, *Climate Change 2001: Impact, Adaptation, and Vulnerability*, Cambridge University Press, Cambridge. UK, 2001.

[6] N. Brook, "Vulnerability, risk and adaptation: a conceptual framework," Working Paper 38, Tyndall Centre for Climate Change Research, University of East Anglia, Norwich, UK, 2003.

[7] J. A. David, J. D. Andrew, and C. S. Lindsay, "Using principal component analysis for information-rich socio-ecological vulnerability mapping in Southern Africa," *Applied Geography*, vol. 35, no. 1-2, pp. 515–524, 2012.

[8] X. Ying, G. M. Zeng, G. Q. Chen, L. Tang, K. L. Wang, and D. Y. Huang, "Combining AHP with GIS in synthetic evaluation of eco-environment quality—a case study of Hunan Province, China," *Ecological Modelling*, vol. 209, no. 2–4, pp. 97–109, 2007.

[9] H. J. de Lange, S. Sala, M. Vighi, and J. H. Faber, "Ecological vulnerability in risk assessment—a review and perspectives," *Science of the Total Environment*, vol. 408, no. 18, pp. 3871–3879, 2010.

[10] X. M. Li, M. Min, and C. F. Tan, "The functional assessment of agricultural ecosystems in Hubei Province, China," *Ecological Modelling*, vol. 187, no. 2-3, pp. 352–360, 2005.

[11] X. J. Li, J. Peterson, G. J. Liu, and L. Qian, "Assessing regional sustainability: the case of land use and land cover change in the middle Yiluo catchment of the Yellow River Basin, China," *Applied Geography*, vol. 21, no. 1, pp. 87–106, 2001.

[12] P. Klungboonkrong and M. A. P. Taylor, "A microcomputer-based system for multicriteria environmental impacts evaluation of urban road networks," *Computers, Environment and Urban Systems*, vol. 22, no. 5, pp. 425–446, 1998.

[13] Z. Qiao and X. L. Xu, "Assessment of soil erosion sensitivity and key factors identification in the Wood-Grass ecotone of northeast China," *Journal of Natural Resources*, vol. 27, no. 8, pp. 1349–1361, 2012.

[14] G. B. Song, Y. Chen, and M. R. Tian, "The ecological vulnerability evaluation in southwestern mountain region of China based on GIS and AHP method," *Procedia Environmental Sciences*, vol. 2, pp. 465–475, 2010.

[15] J. Liu, M. Liu, H. Tian et al., "Spatial and temporal patterns of China's cropland during 1990–2000: an analysis based on Landsat TM data," *Remote Sensing of Environment*, vol. 98, no. 4, pp. 442–456, 2005.

[16] M. R. Rahman, Z. H. Shi, and C. Chongfa, "Soil erosion hazard evaluation—an integrated use of remote sensing, GIS and statistical approaches with biophysical parameters towards management strategies," *Ecological Modelling*, vol. 220, no. 13-14, pp. 1724–1734, 2009.

[17] K. Meusburger, N. Konz, M. Schaub, and C. Alewell, "Soil erosion modelled with USLE and PESERA using QuickBird derived vegetation parameters in an alpine catchment," *International Journal of Applied Earth Observation and Geoinformation*, vol. 12, no. 3, pp. 208–215, 2010.

[18] J. R. Williams, S. L. Neitsch, and J. G. Arnold, *Soil and Water Assessment Tool—User's Manuam*, Blackland Research Center, Texas Agricultural Experiment Station, Texas, Tex, USA, 1999.

[19] S. Q. Wang and C. H. Zhou, "Estimating soil carbon reservoir of terrestrial ecosystem in China," *Geographical Research*, vol. 18, no. 4, pp. 349–356, 1999.

[20] D. W. Lefever, "Measuring geographic concentration by means of the standard deviational ellipse," *The American Journal of Sociology*, vol. 32, no. 1, pp. 88–94, 1926.

[21] J. X. Gong, "Clarifying the standard deviational ellipse," *Geographical Analysis*, vol. 34, no. 2, pp. 155–167, 2002.